Clear-Air Roll Vortices and Turbulent Motions as Detected with an Airborne Gust Probe and Dual-Doppler Radar

R. F. REINKING,[1] R. J. DOVIAK[2] AND R. O. GILMER[1]

Environmental Research Laboratories/NOAA

(Manuscript received 11 August 1980, in final form 27 February 1981)

ABSTRACT

A case-study comparison is made of simultaneous airborne gust probe and dual-Doppler radar measurements of motions associated with roll vortices in the optically clear planetary boundary layer. Intercomparison of the cross-roll component of motion is emphasized. Some similarities and some differences in the data obtained with the two systems are discussed. Considering the differences in measurement techniques, agreement is good between the independent depictions of the roll structure and quantitative determinations of the intensities and predominant scales of eddy motion. The observed roll vortices fit descriptions and cause-effect relationships from certain models and other observations.

1. Introduction

An airborne gust probe and two ground-based Doppler radars were employed to simultaneously measure eddy motions within approximately the same volume of the planetary boundary layer (PBL). The measurements were made on a clear spring afternoon over gently rolling terrain in Oklahoma. Surface heating and moderately strong advection with considerable speed shear in the lower 500 m prevailed. These phenomena induced slight convective instability and longitudinal roll vortices. The vortices were aligned roughly parallel to the wind shear vector, about 20° clockwise from the mean wind (Doviak and Berger, 1980). The roll circulation and superimposed turbulent motions were detected by both measurement systems. In this paper the meteorological conditions that sustained the roll vortices are described, and the intensities and scales of primarily the crosswind component of eddy motions in the rolls, as measured by the independent techniques, are presented and compared.

2. The two methods of measurement

The airborne gust-probe system is used to measure *in situ* the three orthogonal components of perturbation motions (u', v', w') and associated eddy fluxes of momentum, water vapor and sensible heat, in approximately the 10 m–15 km wavelength band. Gust-probe measurements are made at a rate of 80 samples per second in straight horizontal flight. "Instantaneous" and path-average data are obtained. The gust-probe system has been extensively used and proven on large, stable aircraft platforms such as the NOAA DC-6 and WP-3D (Bean *et al.*, 1972, 1975, 1976[3]; Brown *et al.*, 1974). The sensors for the airborne system include the two vanes and pitot tube of the gust probe to measure the wind fluctuations in three dimensions relative to the aircraft, and a microwave refractometer, a thermistor and a pressure transducer to measure absolute humidity and temperature. Accelerometers, and either an inertial navigation system (INS) or a 3-axis rate gyro are used to separate aircraft motions from the gust probe measurements of atmospheric motions. Standard procedures for processing the gust probe data are described by Grossman and Bean (1973)[4] and Bean *et al.* (1976).[3]

The measurements used here were among the first taken with the gust probe mounted on a small twin-engine aircraft, in this case a Beechcraft Model 60 "Duke" (Gilmer *et al.*, 1978)[5]. An economical 3-axis rate gyro, rather than a more sophisticated

[1] Boundary Layer Dynamics Group, Boulder, CO.
[2] National Severe Storms Laboratory, Norman, OK.

[3] Bean, B. R., R. O. Gilmer, R. F. Hartmann, R. E. McGavin and R. F. Reinking, 1976: Airborne measurement of vertical boundary layer fluxes of water vapor, sensible heat and momentum during GATE. NOAA Tech. Memo. ERL WMPO-36, 83 pp. [Govt. Printing Office 1977-799-072].

[4] Grossman, R. L., and B. R. Bean, 1973: An aircraft investigation of turbulence in the lower layers of a marine boundary layer. NOAA Tech. Rep. ERL 291 WMPO 4, 166 pp. [Govt. Printing Office, 1974-784-574/1244].

[5] Gilmer, R. O., R. E. McGavin and R. F. Reinking, 1978: A small aircraft gust-probe system for studies of boundary layer convection and transport. *Preprints Fourth Sym. Meteor. Observation and Instrumentation*, Denver, Amer. Meteor. Soc., 426–432.

INS, was used to correct for aircraft motions. The instrumental root sum square error in measurement of the wind fluctuations with the gyro system is about ± 12 cm s^{-1} under turbulent conditions (based on manufacturer's specifications)[5]; this is about twice the instrumental error experienced with the INS system.[4] The measurement of temperature and moisture is the same with either system. Absolute accuracy in the temperature measurement is approximately $\pm 0.05°C$ with corrections for dynamic heating applied. The resolution in water vapor density ρ_v is better than ± 0.01 g m^{-3}, and the absolute accuracy is about ± 0.2 g m^{-3}. The signals from the various sensors were fed through identical, low-pass 4-pole Butterworth filters with the 3 dB point at 12 Hz, to remove aircraft noise. The signals were then multiplexed, digitized and recorded at the 80 s^{-1} rate, during flights at 85 m s^{-1} along paths some 20 km long. The flights were made approximately perpendicular to the roll vortices ($\sim 20°$ off the perpendicular to the mean wind) as shown by examples in Fig. 1. Subsequently, the data were linearly detrended to remove mean values, and were smoothed to 20 s^{-1} for analysis of the statistical properties, including the sample variance, of the time series records. The samples were further smoothed to 5 s^{-1} for spectral analysis of the scales of motion, to produce power spectra that substantially overlap the 1–16 km band observed by the radars.

A review of dual-Doppler radar observations of clear air PBL wind motions was made in conjunction with new analyses by Berger and Doviak (1979).[6] Doviak and Jobson (1979) reported the first observations of clear air wind perturbations using dual-Doppler radar echos from intrinsic scatterers; e.g., the radars can detect scatter from refractive index fluctuations related to gradients in temperature and absolute humidity. Doviak and Berger (1980) describe the components of the Doppler radars and operating parameters for each on the day when the data for this comparison were taken. They also describe the methods of analysis. The radar resolution volume is a truncated cone some 350–700 m in diameter and 180 m in length for the 25–50 km ranges used in this study. The radar data (mean Doppler velocity, reflectivity, velocity variance, etc.) are interpolated to Cartesian grid points spaced 500 m on surfaces parallel to the plane tangent at the midpoint of the great circle path between the Norman (NRO) and Cimarron (CIM), Oklahoma radar sites indicated in Fig. 1.

The intercomparison set of radar and aircraft data allowed primarily for calculations of u' and v' from the dual-Doppler radar measurements, and v' and w' from the airborne gust probe measurements, although some analyses of the third component from each system were possible. Mainly, the characteristics of the common parameter v', the crosswind component of motion, are considered here; the other components are briefly discussed.

3. Meteorological conditions

The roll observation and instrument intercomparison experiment was conducted on 27 April 1977 (Julian Day 117) in the vicinity of Chickasha, Oklahoma (CKS in Fig. 1), between 1425 and 1500 CST. Dry northerly airflow prevailed on the previous day. Then the winds shifted and strong, steady southwesterly flow brought a continuous low-level influx of moisture from the Gulf of Mexico. The first significant boundary-layer mixing of the day was detected with the radars around 1300 CST. At this time diurnal warming was still in progress and the humidity was gradually increasing (surface observations were 27.4°C and 37% at Will Rogers Airport in Oklahoma City).

Radiosondes were released from Fort Sill, ~50 km southwest (upwind) of Chickasha shortly before and after the experiment (see Fig. 2 of Doviak and Berger, 1980); an aircraft sounding of temperature and moisture was made immediately prior to the turbulence measurements, and temporally continuous surface to 444 m measurements were taken from the NSSL-instrumented KTVY tower in Oklahoma City (Fig. 2). Together these indicate a boundary layer of ~1.1–1.2 km depth (z_i) from about 1300–1400 CST, subsequently deepening to ~1.5 km AGL by about 1500 CST. The boundary layer was thermodynamically slightly stable before 1300 CST but evolved to a nearly adiabatic structure above a shallow superadiabatic surface layer during the intercomparisons. The aircraft encountered nonturbulent air above a shallow inversion layer at z_i and bumpy air in the mixing layer below. Hourly averages of potential temperature lapse rate determined from the tower measurements between 1300 and 1500 CST were steady at 0.06°C $(100\ m)^{-1}$; i.e., potential temperature slightly decreased upward, indicating slight convective instability. A calculated value of -2.25 for the stability parameter z_i/L (L = Monin-Obukov length) also indicated slight convective instability in the mixing layer (Berger and Doviak, 1979).[6]

Vertical profiles of horizontal winds measured with the radars and the instrumented tower reveal little directional shear, with a net veer of about 10° from the surface to 1.5 km AGL, as shown in Fig. 3 of Doviak and Berger (1980). However, these profiles also show that the speed shear was substantial

[6] Berger, M. I., and R. J. Doviak, 1979: An analysis of the clear air planetary boundary layer wind synthesized from NSSL's dual Doppler radar data. NOAA Tech. Memo. ERL NSSL-87, 55 pp. [Govt. Printing Office 1979-0-677-0721 1290].

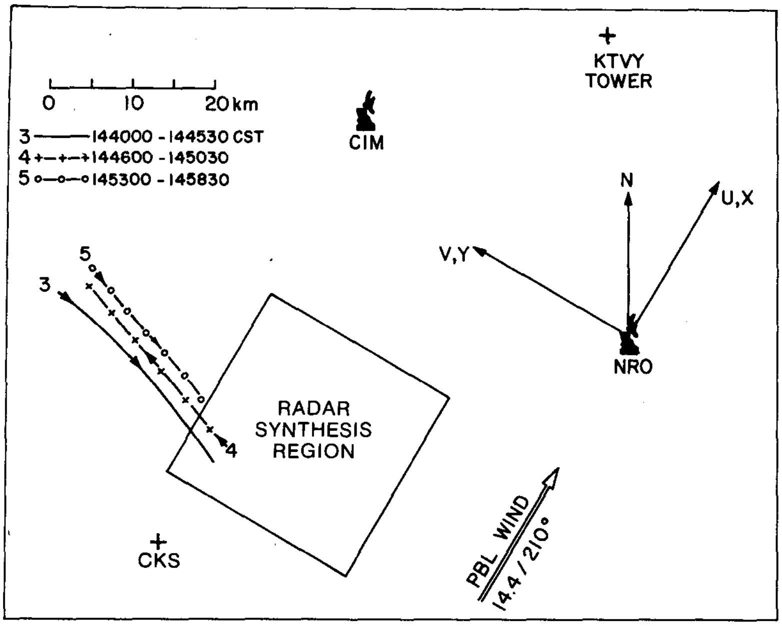

FIG. 1. Plan-view schematic of radar sites and synthesis region observed by the radars, and examples of radar-tracked measurement legs of the instrumented aircraft.

near the ground (~4 m s^{-1} between the surface and 0.1 km, and an additional 2 m s^{-1} between 0.1 and 0.5 km). In the kilometer above 0.5 km AGL the speed decreased by ~1 m s^{-1}. Mean winds at the 1 km flight level were nearly 15 m s^{-1} from 212°.

4. The roll vortices and instrument intercomparisons

Hodographs of the mean horizontal winds observed on the KTVY tower for the period 1300–1600 CST have shapes similar to the wind hodographs produced from the analytical model developed by Brown (1970), such that the profiles in Fig. 3 sug-

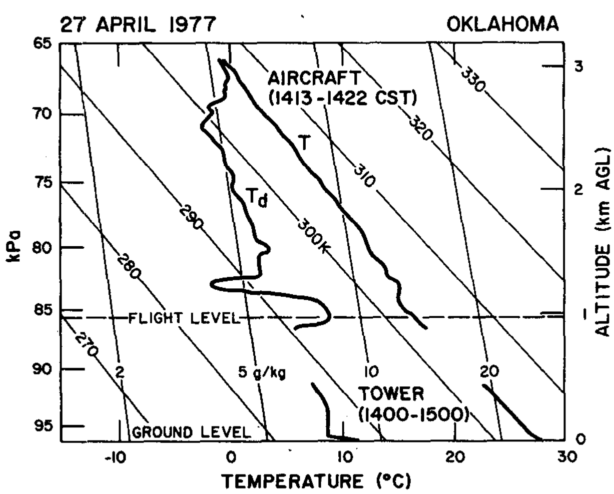

FIG. 2. Aircraft sounding and corresponding, hour-average KTVY tower profile of temperature and moisture (dew point) closest in time to the 1425–1500 CST period of intercomparison measurements.

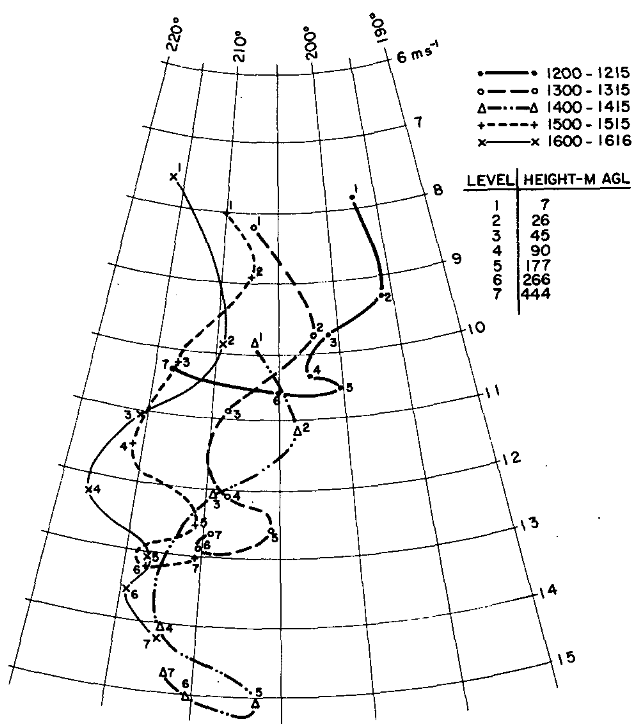

FIG. 3. Hodographs of wind profiles observed before, during and after the period of intercomparison measurements.

gest an Ekman spiral modified by "secondary helical circulations" (roll vortices). The rolls produced by this model are associated with an inflection point of the wind profiled in a plane transverse to the roll axis. Rolls continue to gain energy until the wind profile achieves a shape in which energy gained at one level is balanced by losses at another level. Thus the observed wind profile may be a result of the transfer of energy between rolls and the mean flow.

The clear air rolls, as detected by both the airborne gust-probe system and the dual-Doppler radar system, are depicted in Fig. 4 and the following analyses. Fig. 4a shows the rolls revealed as streets of high reflectivity on the PPI display of one of the 10 cm radars. Fig. 4b is a vertical cross section showing v' and w' motions of the rolls, as resolved from the processed radar data.

Features of the same field of rolls within the experimental area, as simultaneously monitored *in situ* by the airborne gust probe, are depicted in the time series records of the turbulence parameters measured in cross-roll flights (Fig. 4c). [The u', or cross-aircraft, along-roll component of motion is least reliable and is presented with a relative scale because it suffered from some apparent contamination from excessive aircraft yaw that could not be effectively filtered out.]

The rolls were aligned about 10–20° clockwise from the mean PBL wind direction of 210° and the roll spacing was predominantly ~4 km but varied from 2–6 km. The average ratio of horizontal roll spacing to depth was about 2.7:1 (Figs. 4a–4c; and Doviak and Berger, 1980). This ratio and the orientation agree with theory and other observations (e.g., LeMone, 1973, 1976). The v' component of motion is of primary interest here; however, the periodicities and repeated patterns in all five turbulence parameters from the gust probe show the roll characteristics (Fig. 4c). Strong horizontal gradients were observed in water vapor density ρ_v and temperature T; some were at least as large, respectively, as 4 g m^{-3} and 0.8°C in 200 m (Fig. 4c). The magnitudes of these gradients in ρ_v and T along the horizontal are consistent with nonuniformities expected to result from vertical transport between the mixing layer and the zone of the temperature inversion with the corresponding strong vertical gradient in moisture observed in the sounding (Fig. 2). The strong negative correlation between ρ_v' and T' that is evident in Fig. 4c persisted on all of the flight legs.

Alternating with periods (zones) of strong fluctuations in ρ_v' and T' are periods with minimal fluctuation in either parameter (Fig. 4C). The latter periods are suggestive of well-mixed air transported within the cores of the better-defined rolls where both moderately rising and sinking air was encountered

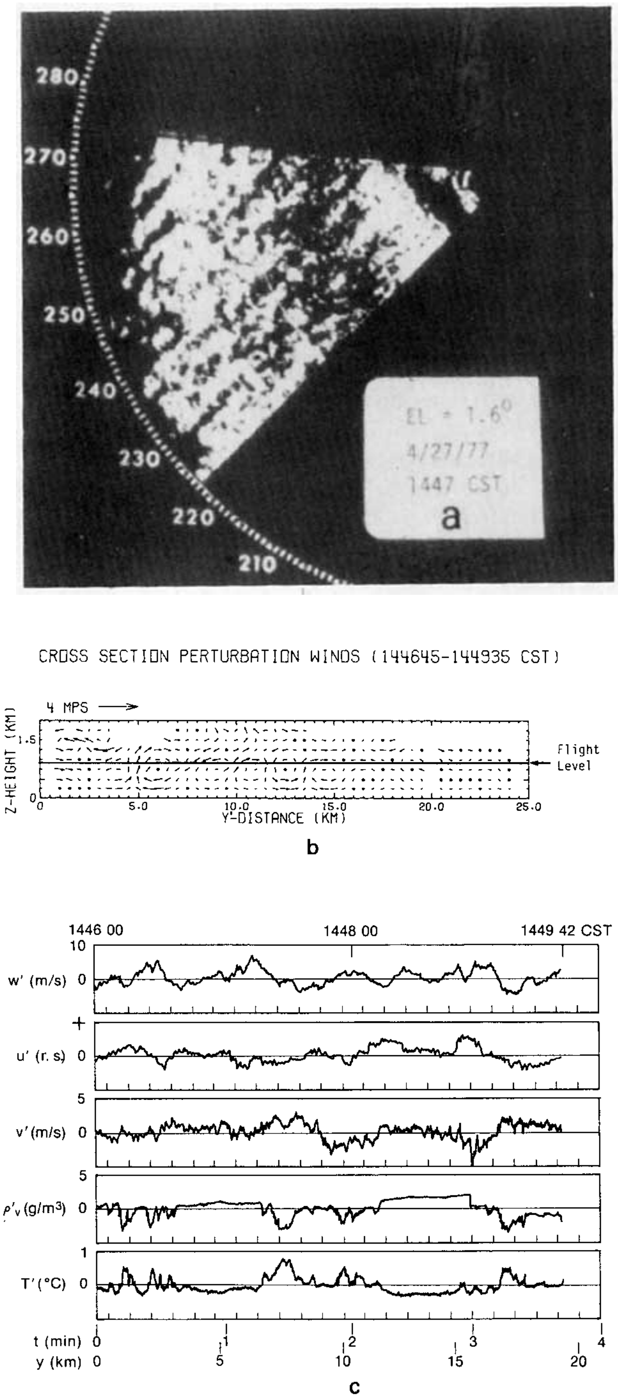

FIG. 4. (a) PPI contour display of reflectivity × R^{-2} (R is range) from Norman, Oklahoma Doppler radar. Bright areas of higher reflectivity are aligned 10–20° clockwise from the mean wind and the bands are spaced ~4 km apart. Intervals between range arcs are 20 km. (b) Vertical cross section of v' and w' components of motion from dual-Doppler radar observations. Aircraft flight level in the same vicinity is indicated. (c) Time series records of eddy motions and absolute humidity and temperature fluctuations measured with the airborne gust probe at same time as radar observations.

(note flight level relative to axes of rolls in Fig. 4b), or of well-mixed air rising more vigorously from lower levels, between rolls.

The strong fluctuations in moisture and temperature indicate nonuniform mixing of air from different sources, i.e., from within and above the mixing layer. In these zones, ρ_v' is predominantly negative and T' is positive. This suggests that warm, dry air was indeed being entrained downward from the temperature inversion. Other investigations have shown that this process can cause ρ_v' and T' to be negatively correlated in the entire upper half of the mixing layer, where the strength of the correlation increases upward to the capping inversion (e.g., Wyngaard *et al.*, 1978). Taken collectively, the time series from the several flight legs show that at least the more strongly sinking air was warm and dry. The corresponding correlations of moisture and temperature with vertical motion ($w'\rho_v'$ positive, $w'T'$ negative) are not pure, i.e., they did not exist everywhere along the flight paths, presumably because the well-defined rolls were interspersed with less organized circulations (Fig. 4b), and the vertical structure of the atmosphere was probably not horizontally uniform.

Some comparisons of the gust-probe and radar observations are now made. Large gradients such as those observed in temperature and moisture were evidently mixed by turbulence to produce fluctuations in ρ_v and T at centimeter scales, to cause the irregularities and strong gradients in refractive index sensed by the radars (e.g., Fig. 4a). Excellent agreement, within 1 dB, between refractive index structure constants (Tatarski, 1961) of the clear air determined independently from these radar and aircraft measurements (Doviak and Berger, 1980) gives credence to this interpretation of radar targets.

The intensities, or variances, of the cross-roll eddy motions $\sigma_{v'}^2$ from the aircraft and radar measurements are compared as a function of sampling times in Fig. 5. One flight leg at constant altitude constitutes an aircraft sample; one volume scan focused on the same altitude constitutes a radar sample. Sample-by-sample, this variance as measured with the gust probe was usually somewhat greater than the values measured with the dual-Doppler radar. The composite means for all samples are $\overline{\sigma_{v'}^2}$ (gust-probe) = 1.30 and $\overline{\sigma_{v'}^2}$ (Doppler) = 1.17 $m^2 s^{-2}$; the average ratio of paired values is 1.05. Thus the difference between intensities of v' determined by the two systems is of the order of 5–10% in the mean. The variance of flight path velocities measured by aircraft is expected to be larger than the variance of volume-averaged velocities measured by radar (Doviak and Berger, 1980).

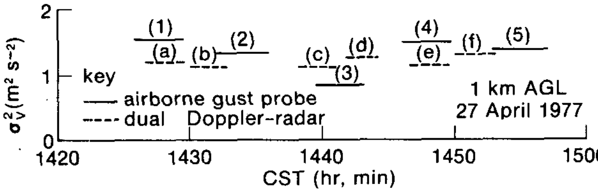

FIG. 5. Variance of the cross-roll component of motion, v', as measured by the airborne gust probe (samples 1–5) and the dual-Doppler radar (samples a–f). Sampling time periods are indicated by the bars.

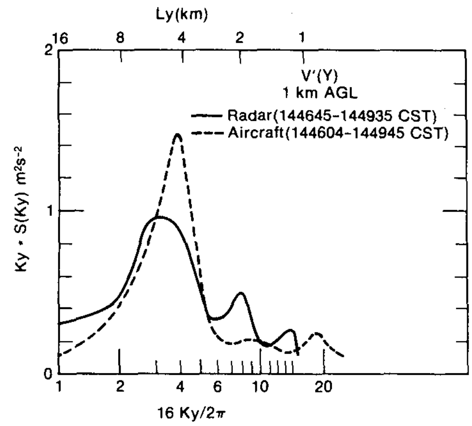

FIG. 6. Example of time-coincident power spectra of v' at 1 km AGL from dual-Doppler radar and gust-probe measurements. The spectrum deduced by radar is an average of 16 one-dimensional spectra within the radar synthesis region for the time the aircraft was flying path 4.

Fig. 6 is an example of the power spectra of v' calculated for the individual, paired gust-probe and radar samples. The aircraft sample pathlengths were shorter than desirable to establish good statistical confidence in the power spectra for the principal scales of motion encountered. Confidence in the measurements comes mainly from the clear depiction of the rolls in the time/space domain from both sets of observations (e.g., Fig. 4) and the agreement between the aircraft and radar spectra in individual and composite forms. The spectra for the individual, paired samples (e.g., Fig. 6) agree as closely as is reasonably possible, considering the basic difference of the aircraft line-path measurements versus the dual-Doppler radar volume-averaged data interpolated to grids at the same altitude (1 km AGL). Some secondary peaks in both the aircraft and the radar spectra show variable effects of convection and turbulence on motion scales smaller than those of the rolls.

The spectral variance in v' for each gust probe sample is concentrated primarily in the 1–8 km band. Likewise, the variance from the radar measurements consistently reaches its peak well within the 1–16 km wavelength band, and then diminishes to small values at those band limits. Spectral powers calculated across this band reflect the aforementioned mean difference of only 5–10% in total variance and are thus comparable for the two systems. The peak spectral powers average ~0.75 $m^2\ s^{-2}$ with a standard deviation of $\pm 0.35\ m^2\ s^{-2}$ for the aircraft and $\sim 0.85 \pm 0.15\ m^2\ s^{-2}$ for the radar. Thus, radar spectra are for the most part smoother and more constant from sample to sample than the spectra from the airborne measurements, because the former are grid averages of 16 one-dimensional spectra taken along parallel lines in the y direction at the 1 km altitude. The predominant scales of the v' component of motion determined from the individual spectra vary within a 3–5 km range for the gust-probe samples and a 4–6 km range for the radar samples.

This good agreement between aircraft and radar measurements is upheld in composites of the individual v' spectra which provide space-time averages that are perhaps the most suitable for comparison (Fig. 7). The composite spectrum of the five gust probe samples in Fig. 5 shows a predominant scale of cross-roll motion of ~4.5 km in agreement with the composite spectrum of the six dual Doppler radar samples. Between approximately the 4 and 10 km scales, the radar-measured variance (area under the curve) was somewhat larger than that measured with the gust probe. The gust-probe composite shows a minor peak near 1.5 km; similar scales also were seen in individual cases with the radar (e.g., Fig. 6) but did not carry through to the composite; at scales shorter than 4 km the variances are otherwise nearly identical. Some contributions to the total aircraft-measured variance are made by scales shorter than the 1 km cutoff of the radar band. Overall, considering the aforementioned differences in the systems, some spatial offset in the volumes of the boundary layer examined (Fig. 1) and some temporal offsets of a few minutes in the samples (Fig. 5), the composite spectra of v' compare well.

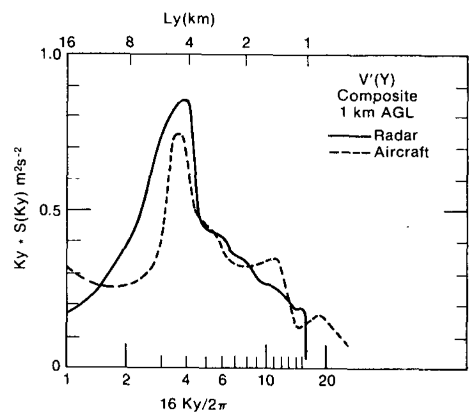

FIG. 7. Composites of spectra of v' measured with the gust probe and the dual-Doppler radar.

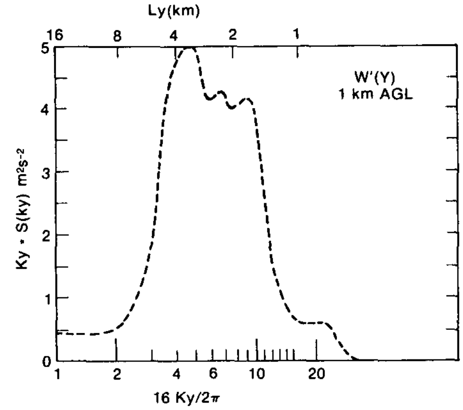

FIG. 8. Composite of five spectra of vertical eddy motion measured in cross-roll flight with the gust probe.

Some notes on the other components of motion are now made. The time series of the vertical component of motion (w', Fig. 4c) also depicts the roll structure resolved by the gust-probe system. There appears to be a 90° phase shift between w' and v', as expected for rolls. A composite mean power spectrum from the five flight legs made within the experimental period indicates a predominant scale of vertical eddy motion of 3.6 km (Fig. 8). The corresponding composite mean variance or intensity of vertical motion, $\overline{\sigma_{w'}^2}$, is 6.4 $m^2\ s^{-2}$. The peak-to-peak magnitudes of w' in the time series and the corresponding principal scale in the spectrum are similar to those observed in other case studies of rolls (e.g., Bean *et al.*, 1975; LeMone, 1976).

The radar derived y-z cross sections of vertical and cross-roll eddy motions, shown in Fig. 4b, qualitatively agree well with the aircraft time series (Fig. 4c) in depicting the scale of the rolls. Despite this agreement, the spectra $K_y S_w(K_y)$ of vertical velocities derived from integrating radar-measured horizontal divergence from the surface-to-flight altitude, did not agree with the spectra measured by aircraft (Fig. 8). Although the spectra from the radars showed peaks at the roll wavelength for a few cross sections, these peaks had amplitudes considerably less than that shown in Fig. 8. Furthermore, averages of the radar spectra over 16 y-z cross sections showed no evidence of a spectral peak at roll wavelengths but a spectral shape that suggested noise may have been dominating the divergence measurements at lower altitudes. (By comparison, the rolls depicted in Fig. 4b are from a vertical plane rather than an average over all cross-sectional planes.) This hypothesis could not be tested because simultaneous aircraft and radar measurements to compare horizontal winds below the 1 km flight altitude were not obtained. Also, the radar did not sample the horizontal winds below ~250 m AGL, and cannot sample much below 150 m at ranges used in this experiment; thus divergence measurements near the surface, important to the calculation of the vertical velocities, may have been missed. Consequently, the vertical velocity perturbations determined from the radars are less reliable than the horizontal ones.

Spectra of u', the alongwind component of eddy motion, derived from the dual-Doppler radar data show a peak at about the same scale but with much smaller magnitude than that exhibited by the spectrum of v'. The roll phenomenon also is indicated in the structure of u' from the gust-probe measurements (Fig. 4c), despite some aforementioned contamination of this cross-aircraft component from incompletely filtered yaw which may have affected the measurements of scales of this motion on some of the flight legs. The rolls, churning in the presence of the large vertical shear in $\bar{u}$, vertically displace u momentum; hence u' perturbations should have a periodicity equal to roll wavelength, as indicated by both systems.

5. Conclusions

The observed quasi-steady state system of deep, clear air roll vortices and the sustaining meteorological conditions fit descriptions determined from certain models and other observations. The rolls developed in an inversion-capped PBL with slight convective instability. The system was driven by surface heating and moderately strong, persistent advection with considerable speed shear near the ground. Wind profiles indicate Ekman spirals modified as anticipated by the helical circulations. Roll spacing averaged ~4 km, and alignment was slightly clockwise from the mean PBL wind and parallel to the shear vector.

The airborne gust-probe system and the dual-Doppler radar system qualitatively and quantitatively agreed very well in independent characterizations of the roll vortices. Predominant scales of crosswind (cross-roll) eddy motion of some 3–5 km were clearly determined by both systems, and the measured intensities of motion, $\sigma_{v'}{}^2$, agreed within 5–10% in the mean, despite the small number of samples available for comparison. While the vertical and alongwind components of motion, w' and u', could not be thoroughly compared in this particular case study, separate analysis of differing types, such as time series and a power spectrum of w' from the gust probe, and a vertical cross section PBL wind field from the radars, are consistent in depicting the roll structure. Although the number of samples examined is small, the results are definitely encouraging.

The two instrument systems are in certain respects complementary. The measurements from one can help to substantiate those from the other, as demonstrated here. When the refractive index structure constant is about 10^{-12} $m^{-2/3}$ or greater, the dual-Doppler radars can measure the PBL eddy motions in three dimensions over a large study area (~10 000 km^2), and in much less time than required to obtain a few line path measurements with the aircraft. This is a major advantage. Also, considering the long aircraft path lengths required to obtain representative spectra, the radar is better adapted to measure the wavelengths or scales of motion larger than a few kilometers.

Conversely, the airborne gust probe can be used to measure turbulence on scales as small as ~10 m if needed, whereas the short-wavelength cutoff of the 10 cm dual-Doppler radar is ~1.0 km. Turbulence occurring as low as ~15 m above highest terrain can be measured with the aircraft, whereas the minimum altitude for radar measurements is range-dependent and higher (e.g., ~150 m at ~50 km). The airborne sampling takes place *in situ*, without interference from unwanted "intrinsic scatterers" such as insects or birds; it also can obtain data when the PBL is so well mixed or stable that it lacks the temperature and moisture (refractive index) perturbations required for good radar returns. This difference was demonstrated when both systems were operated in a field of rolls and small cumuli on a relatively moist day subsequent to the case presented above: On 29 April 1977 the aircraft clearly detected good roll structure and subcloud convection at 0.5 km AGL, but measured *in situ* absolute humidity gradients of only ~0.5 g m^{-3} in 200 m (compared to ~4.0 g m^{-3} in 200 m gradients on the day of the above comparisons). The former gradients were insufficient to generate radar reflectivities strong enough for Doppler velocity measurements.

Both systems offer some advantages over tower measurements, particularly in non-steady-state boundary layers, or in the presence of quasi-stationary rolls such as those observed. Further comparisons with more substantial data sets are warranted.

Acknowledgments. Dr. B. R. Bean, Chief of BLDG, conceived and directed the experiment. M. I. Berger, now with the National Weather Service in Minneapolis, and R. Rabin of NSSL contributed to the analysis of the dual-Doppler radar data. R. E. McGavin and R. F. Hartmann were instrumental in analyzing the data from the airborne gust probe.

REFERENCES

Bean, B. R., C. B. Emmanuel, R. O. Gilmer and R. E. McGavin, 1975: The spatial and temporal variations of the turbulent fluxes of heat, momentum and water vapor over Lake Ontario. *J. Phys. Oceanogr.*, **5**, 532–540.

——, R. Gilmer, R. L. Grossman, R. McGavin and C. Travis, 1972: An analyses of airborne measurements of vertical water vapor flux during BOMEX. *J. Atmos. Sci.*, **29**, 860–869.

Brown, R. A., 1970: A secondary flow model of the planetary boundary layer. *J. Atmos. Sci.*, **27**, 742–757.

Brown, W. J., Jr., J. D. McFadden, H. J. Mason, Jr. and C. W. Travis, 1974: Analysis of the Research Flight Facility gust probe system. *J. Appl. Meteor.*, **13**, 156–167.

Doviak, R. J., and M. I. Berger, 1980: Turbulence and waves in the optically clear air planetary boundary layer resolved by dual-Doppler radars. *Radio Sci.*, **15**, 297–317.

——, and C. T. Jobson, 1979: Dual-Doppler radar observations of clear air wind perturbations in the planetary boundary layer. *J. Geophys. Res.*, **84**, 697–702.

LeMone, M. A., 1973: The structure and dynamics of horizontal roll vortices in the planetary boundary layer. *J. Atmos. Sci.*, **30**, 1077–1091.

——, 1976: Modulation of turbulence energy by longitudinal rolls in an unstable planetary boundary layer. *J. Atmos. Sci.*, **33**, 1308–1320.

Tatarski, V. I., 1961: *Wave Propagation in a Turbulent Medium* (Transl. by R. A. Silverman). McGraw Hill, 285 pp.

Wyngaard, J. C., W. T. Pennell, D. H. Lenschow and M. A. LeMone, 1978: The temperature-humidity covariance budget in the convective boundary layer. *J. Atmos. Sci.*, **35**, 47–58.